Phys. Med. Biol. **42** (1997) 2411–2420. Printed in the UK PII: S0031-9155(97)83529-4

Dose optimization of proton and heavy ion therapy using generalized sampled pattern matching

Kiyoshi Yoda†‡, Yoshifuru Saito§ and Hidenobu Sakamoto‖

† Mitsubishi Electric Corporation, Advanced Technology R&D Center, 8-1-1 Tsukaguchi-Hommachi, Amagasaki 661 Japan

§ Hosei University, College of Engineering, Department of Electronics & Electrical Engineering, 3-7-2 Kajino, Koganei, Tokyo 184 Japan

‖ Mitsubishi Electric Corporation, Communications Equipment Works 8-1-1 Tsukaguchi-Hommachi, Amagasaki 661 Japan

Received 18 April 1997, in final form 1 September 1997

Abstract. We have proposed a new dose optimization method for proton and heavy ion therapy using generalized sampled pattern matching, where an optimal beam weight distribution for scanning is obtained as a solution. Using water phantom models, one-dimensional lateral and depth dose distributions were separately optimized, each resulting in a uniform dose distribution within a target region and minimum dose fall-off to minimize undesired irradiation onto neighbouring tissues. Subsequently, we have applied the technique to broad beam three-dimensional proton therapy, leading to a homogeneous dose distribution inside a target and minimized distal and lateral dose fall-off for most convex tumour shapes.

1. Introduction

Optimization of proton or heavy ion therapy ideally requires a uniform dose distribution within a target volume, a zero dose level in critical organs, and a minimum dose level in other normal tissues.

Several optimization techniques have been reported using a least-squares method (Pedroni 1995) or an iterative deconvolution scheme (Lind 1988, Brahme *et al* 1989) to obtain beam weight solutions for a given dose distribution. The unconstrained least-squares method may lead to unphysical negative beam weight solutions. The solution also depends on initial values, and it is not always easy to guess good initial values. This initial value problem may be overcome by employing random methods such as simulated annealing; however, this better strategy still has the negative solution problem. Meanwhile, the iterative deconvolution method is not directly applicable for inhomogeneous media, because the formulation is based on convolution of a spatially invariant energy deposition kernel.

We have proposed a new dose optimization method for proton and heavy ion therapy using generalized sampled pattern matching (Saito and Yoda 1996), where the resulting beam weights are always non-negative as for the previous iterative deconvolution scheme, and moreover a heterogeneous medium may be considered once we calculate spatially varying energy deposition kernels using Monte Carlo methods (Goitein and Sisterson 1978) or other

‡ E-mail address: yoda@ele.crl.melco.co.jp

0031-9155/97/122411+10$19.50

approximated formulations such as semi-infinite slab models (Larsson 1987, Russell *et al* 1995). In this report, we show preliminary dose optimization results for homogeneous water phantom models.

2. Principle of generalized sampled pattern matching

Generalized sampled pattern matching (GSPM) is a generalization of an inverse problem solver, sampled pattern matching (Saito *et al* 1990, Saotome *et al* 1993, 1995, Yoda *et al* 1997). The original sampled pattern matching (SPM) provides only a one-bit (0 or 1) solution while the GSPM gives a multiple-bit solution. Here, we describe the GSPM principle using the terminology of three-dimensional proton dose optimization.

The basic equation we want to solve is given as follows:

$$D(\boldsymbol{r}) = \sum_i N_i H_i(\boldsymbol{r}) \tag{1}$$

where $\boldsymbol{r}$ is a three-dimensional spatial position (x, y, z), $D(\boldsymbol{r})$ is the desired dose distribution inside the medium, $H_i(\boldsymbol{r})$ is a dose distribution given by a monoenergetic Gaussian beam often called an energy deposition kernel and N_i is a beam weight or the number of incident particles. In GSPM, the beam weight solution N_is are approximated by quantized discrete values, and therefore the solution process is based on a discrete search algorithm. The GSPM involves two important aspects: unique objective function and a unique solving procedure.

The objective function for the GSPM algorithm is cosine of the vector angle between a desired dose distribution vector $\boldsymbol{U} = (u_1, u_2, \ldots, u_m)$ and a theoretically calculated dose distribution vector $\boldsymbol{V} = (v_1, v_2, \ldots, v_m)$ where m denotes the number of dose sampling points. In other words, each u_i $(i = 1, \ldots, m)$ corresponds to a desired dose $D(\boldsymbol{r}_i)$ in equation (1) that is predetermined, whereas each v_i $(i = 1, \ldots, m)$ corresponds to a theoretically calculated dose given by the right-hand side of equation (1). The cosine of the angle θ of the above two vectors $\boldsymbol{U}$ and $\boldsymbol{V}$ is given by the inner product of the corresponding normalized vectors as follows:

$$\cos\theta = \frac{\boldsymbol{U} \cdot \boldsymbol{V}}{|\boldsymbol{U}||\boldsymbol{V}|} \tag{2}$$

$\cos\theta$ is called the pattern matching index. If the two vectors $\boldsymbol{U}$ and $\boldsymbol{V}$ lie in a same direction, then the value of $\cos\theta$ is 1.0, giving the best pattern matching regardless of the vector amplitudes $|\boldsymbol{U}|$ and $|\boldsymbol{V}|$. Conventional optimization methods always try to minimize the squared sum of the difference between the desired values and the calculated results; consequently, we have to consider absolute dose levels from the beginning possibly leading to undesirable local minimum solutions. In contrast, the GSPM finds a normalized beam weight distribution as a solution thereby highly reducing such local minimum problems. The absolute beam weight or irradiation dose can easily be obtained by dividing the desired absolute dose by the calculated relative dose after the optimization.

The optimization procedure resembles piling building blocks on the floor one-by-one. In this case, we add the individual beams, $H_i(\boldsymbol{r})$ (defined in equation (1)), together in an incremental fashion. Each beam is added with an incremental or unit beam weight (of say 0.1), and the same beam may be added with this incremental weight several times in the procedure if necessary. The first step is to choose one beam from the set of beams $\{H_i(\boldsymbol{r})\}$ that maximizes $\cos\theta$. For example, consider a one-dimensional problem of finding the weighting factors in the superposition of monoenergetic Bragg peaks to obtain a spread-out Bragg peak (i.e. the one-dimensional version of equation (1)). The beam that maximizes

$\cos\theta$ is the most energetic beam (i.e. the beam with the longest range) because for all other beams there will be some terms in the sum $U \cdot V = \sum u_i v_i$ which are zero. The beam with the longest range is the 'most important' beam in the superposition, and it is the one that is recognized first by the pattern matching index. The optimization process continues by adding in beams incrementally such that the pattern matching index, $\cos\theta$, is maximized for each addition step. This is repeatedly performed until all possible beams are included. Finally, we obtain an optimal weight distribution by finding the highest pattern matching index for all the combinations of beams considered.

Figure 1 shows the process of finding the solution. For simplicity a one-dimensional example is shown. The GSPM yields a solution after placing all the possible beam weights as shown in figure 1. The optimal weight distribution is obtained by selecting the distribution with the highest value of $\cos\theta$. This is represented by one of the intermediate diagrams in figure 1. In this figure the incremental or unit beam weight is chosen to be 0.1 and the maximum weight is set at 1.0 thereby providing a 10-step dynamic range for the optimal weight solution. For more precision, we simply choose a smaller unit weight such as 0.01 while maintaining the maximum weight unchanged. All the calculations were initially done by *Mathematica* (Wolfram 1991). Subsequently, the GSPM routine was coded by C and called from inside *Mathematica*.

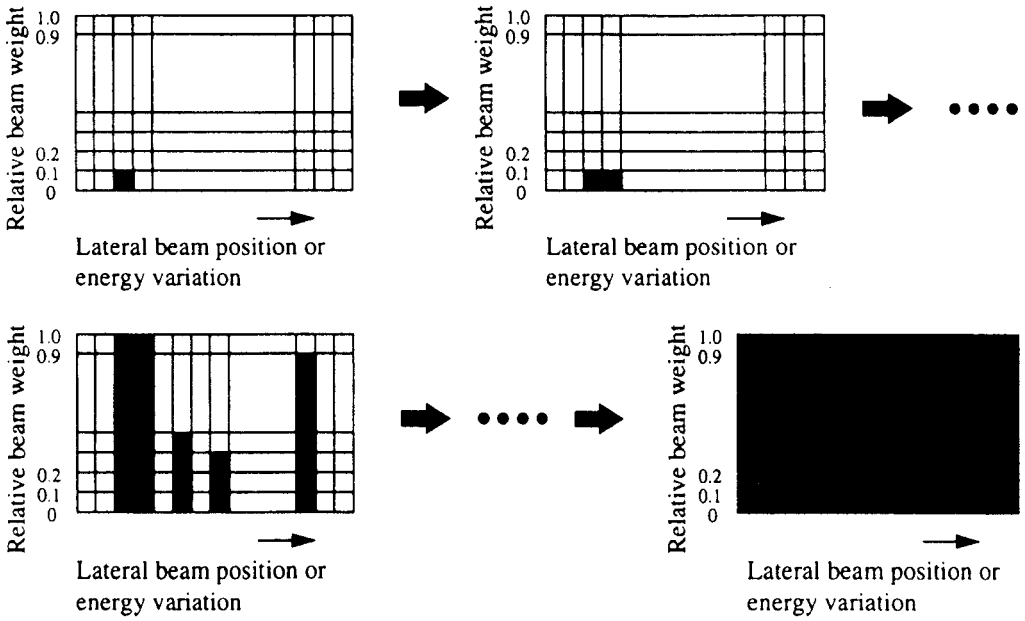

Figure 1. Diagram of solution search processes of generalized sampled pattern matching (GSPM). The solution is given as the beam weight distribution having the highest pattern matching index, $\cos\theta$.

3. Results

3.1. One-dimensional lateral dose optimization

The lateral dose distribution $D(x, z_0)$ at depth z_0 is given as follows:

$$D(x, z_0) = \sum_i N_i \frac{\exp[-(x - i\Delta x)^2/\sigma^2]}{\pi\sigma^2} S(E, z_0) \tag{3}$$

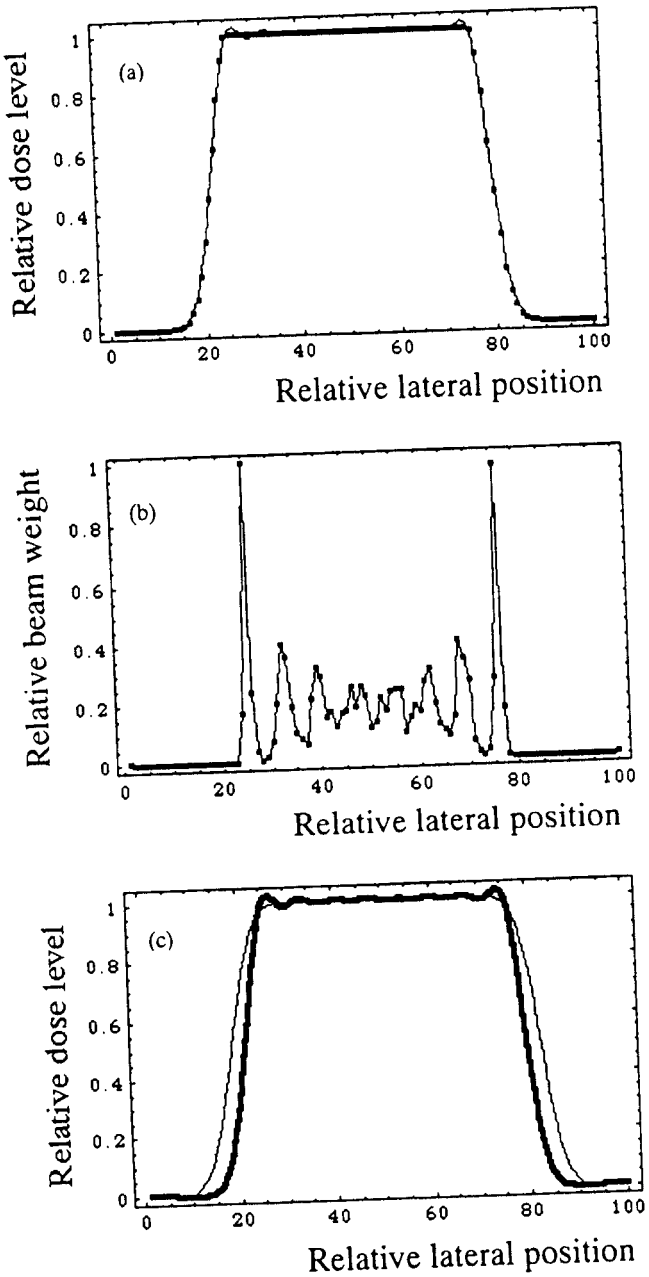

Figure 2. Results of one-dimensional lateral dose optimization: (*a*) the desired beam profile (dots) as compared with the profile obtained by the GSPM procedure (full curve); (*b*) the beam weight pattern required to generate the GSPM dose distribution shown in (*a*); (*c*) the beam profile generated by a uniform beam (thin curve) compared with the profile generated by the GSPM procedure (thick curve).

where x denotes the lateral coordinate, N_i is a beam weight, Δx is a step size for scanning, σ is a $1/e$ beam radius at the depth z_0, and $S(E, z_0)$ is a stopping power at the depth z_0 generated by a broad parallel beam having an initial energy of E.

Figure 2(*a*) shows a desired lateral dose distribution (dots) and the optimized dose distribution (full curve) calculated by the GSPM algorithm, where the desired lateral dose

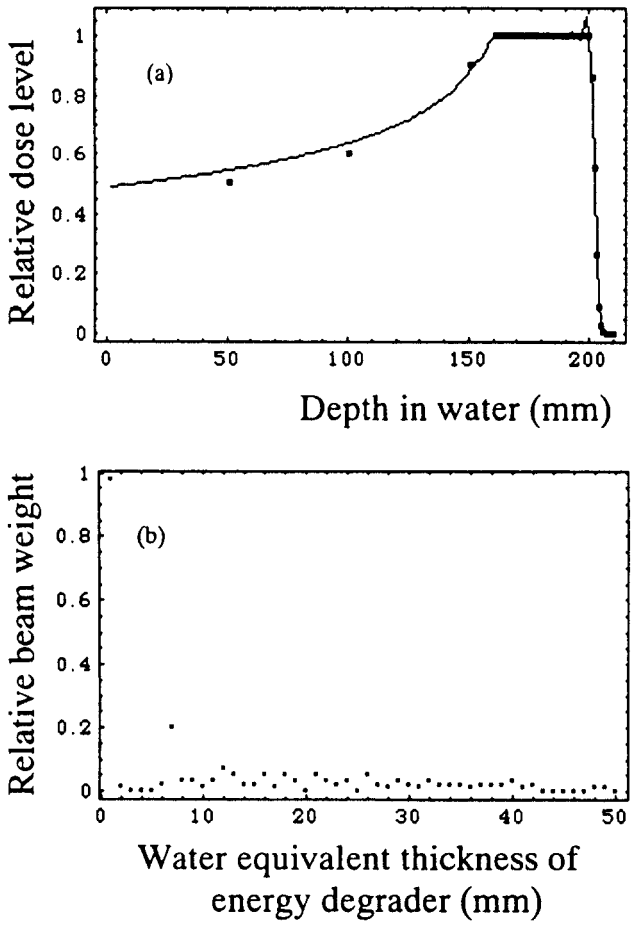

Figure 3. Results of one-dimensional depth dose optimization. (*a*) The desired beam profile (dots) as compared with the profile obtained by the GSPM procedure (full curve). The number of dose sampling points in the uniform region was 40, and thus it looks like a thick line. (*b*) An optimal beam weight solution as a function of energy degrader thickness, where monoenergetic proton beams of 50 different energies with a constant range decrement of 1 mm irradiate a water sample.

fall-off was given by the Gaussian distribution characteristic for a single pencil beam. Figure 2(*b*) depicts the optimal solution (dots) of lateral beam weights. The full curve was drawn only for easier observation. In figure 2(*c*), the optimized dose distribution (thick curve) is compared with the dose resulting from a uniform beam (thin curve). These results indicate that the optimization minimizes the lateral dose fall-off to the physical limit while providing a homogeneous dose inside the target.

3.2. One-dimensional depth dose optimization

The depth dose distribution on a central axis $D(0, z)$ generated by a broad parallel beam is given as follows:

$$D(0, z) = \sum_i N_i S(E_i, z) \tag{4}$$

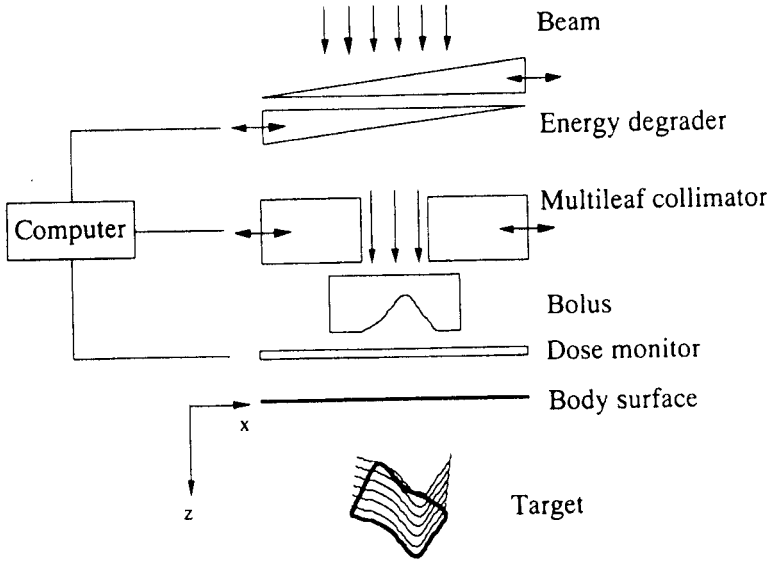

Figure 4. Diagram of the broad beam three-dimensional proton therapy system.

where z denotes the depth coordinate, N_i is a beam weight of an initial energy E_i, and $S(E_i, z)$ is stopping power at the depth z generated by the beam having the initial energy of E_i. In this paper, the relative stopping power has been taken from measurements made on the 187 MeV broad proton beam from the Gustav Werner synchrocyclotron in Sweden (Larsson 1961).

Figure 3(*a*) shows a desired depth dose distribution (dots) and the optimized dose distribution (full curve) using the GSPM procedure, where the desired distal dose fall-off was given by the fall-off of a monoenergetic beam having the same range. Monoenergetic proton beams of 50 different energies with a constant range decrement of 1 mm irradiate a water sample. The number of dose sampling points in the uniform region was 40, and thus it looks like a thick full line. Figure 3(*b*) depicts an optimal beam weight distribution as a function of water equivalent thickness of an energy degrader. The results indicate that the optimization minimizes the distal dose fall-off to the physical limit while giving a homogeneous dose distribution inside the target. The overshoot at the distal corner results from the ideal fall-off characteristic provided as a part of the desired distribution.

As shown in Figure 3(*a*), we placed only three dose sampling points at the plateau region for the desired dose distribution because we do not know the exact dose level in this region beforehand. The GSPM pattern matching procedure utilizes the vector inner product given by equation (2), and therefore the assigned sampling point density automatically corresponds to the weighting coefficient of the pattern matching calculation.

3.3. Application to broad beam three-dimensional proton therapy

Figure 4 shows a diagram of a broad beam three-dimensional proton therapy system (Kanai *et al* 1983a). The broad beam that runs in parallel irradiates a target inside a body through a variable energy degrader, a multileaf collimator, a fixed bolus and a dose monitor. A computer receives dose signals from the dose monitor; subsequently, the computer transmits control signals to the energy degrader and the multileaf collimator during irradiation.

In this system, the treatment volume is layered according to the shape of the distal surface of the target, and the dose is built up using the energy degrader, the multileaf

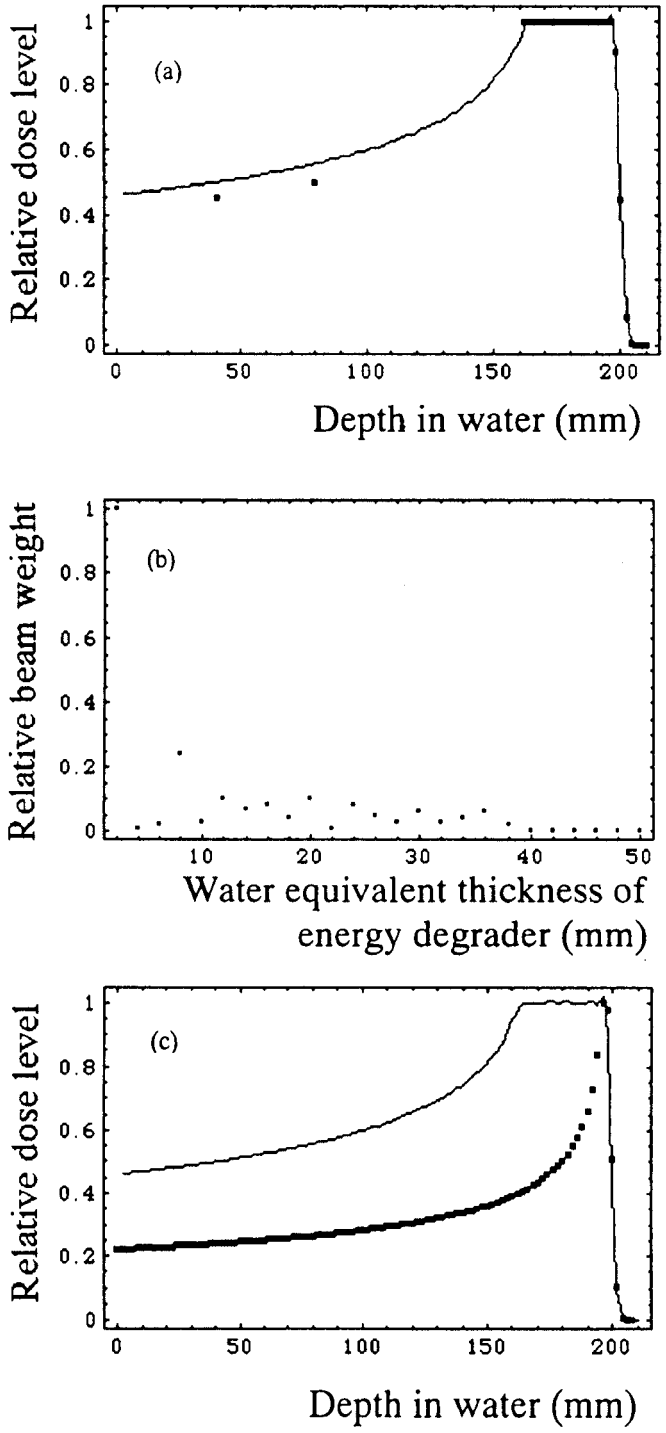

Figure 5. Results of depth dose optimization for the broad beam three-dimensional therapy system. The optimization was performed along the depth-directed line including the deepest point of the target. (*a*) The desired depth dose distribution (dots) is compared with the optimized dose distribution (full curve). The number of dose sampling points in the uniform region was 18, and thus it looks like a thick line. (*b*) An optimal beam weight is shown as a function of energy degrader thickness, where monoenergetic proton beams of 25 different energies with a constant range decrement of 2 mm irradiate a water sample. (*c*) The optimized dose distribution (full curve) is compared with a monoenergetic Bragg curve (dots).

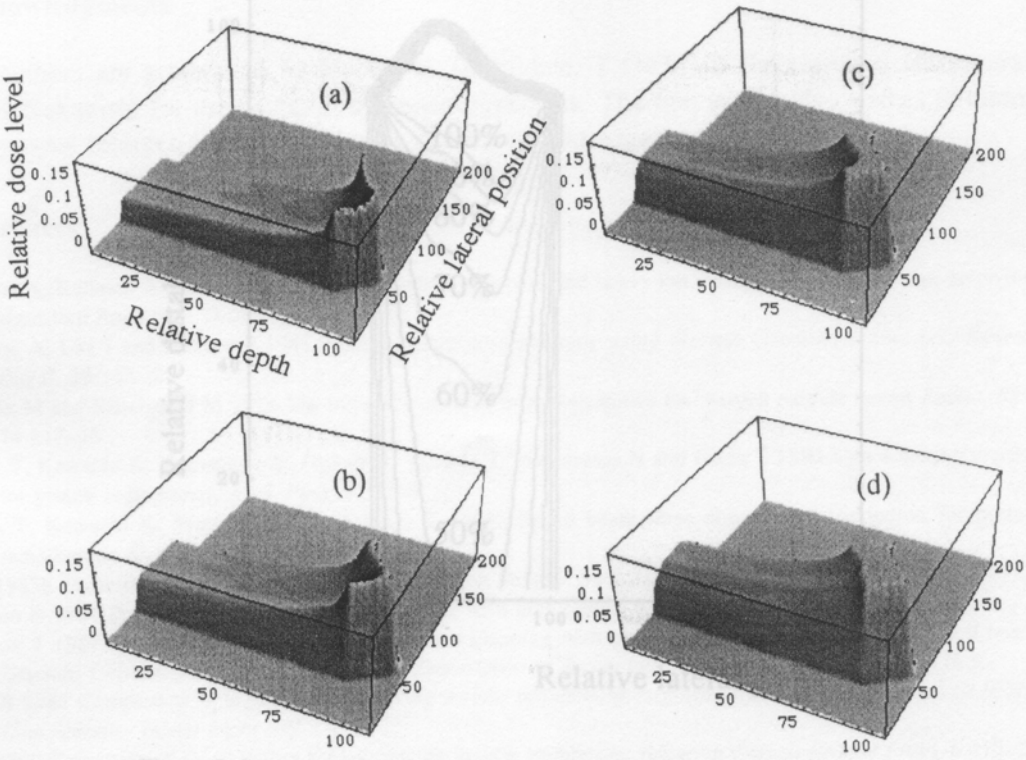

Figure 6. Three-dimensional plots (*a*)–(*d*) of the dose distribution during optimized irradiation.

collimator and the bolus. When the range is shortened by increasing the degrader thickness, the irradiated field aperture is changed using the multileaf collimator to maintain conformal irradiation.

The absorbed dose contribution to a point at depth z and distance x from a central axis of a Gaussian proton beam having an energy E and a beam weight $N(E)$ is given as follows:

$$D(x,z) = N(E)\frac{\exp[-x^2/\sigma(z)^2]}{\pi\sigma(z)^2}S(E,z) \tag{5}$$

where $\sigma(z)$ is a $1/e$ beam radius at the depth z and $S(E,z)$ is a stopping power. In this calculation, the initial $1/e$ radius of the incident Gaussian beam is set at 3 mm, and the beam radius in water has been taken from measurements made on the 177 MeV proton beam from the PSI cyclotron in Switzerland (Scheib *et al* 1994). Further, it is known that a broad collimated beam can be generated by a summation over a finite number of narrow Gaussian beams (Brahme *et al* 1981), and this idea was used for the present calculation. The edge scattering at the collimator wall were ignored for simplicity.

Figure 5(*a*) shows a one-dimensional desired depth dose distribution (dots) and the optimized dose distribution (full curve) using the GSPM procedure, where the optimization was performed along the depth-directed line including the deepest point of the target. The number of dose sampling points in the uniform region was 18, and thus it looks like a thick line. Again the desired distal dose fall-off was given by the fall-off of a monoenergetic beam having the same range. Figure 5(*b*) depicts an optimal beam weight solution as a function of energy degrader thickness. Monoenergetic proton beams of 25 different energies with constant range decrements of 2 mm irradiate the medium. Figure 5(*c*) shows the

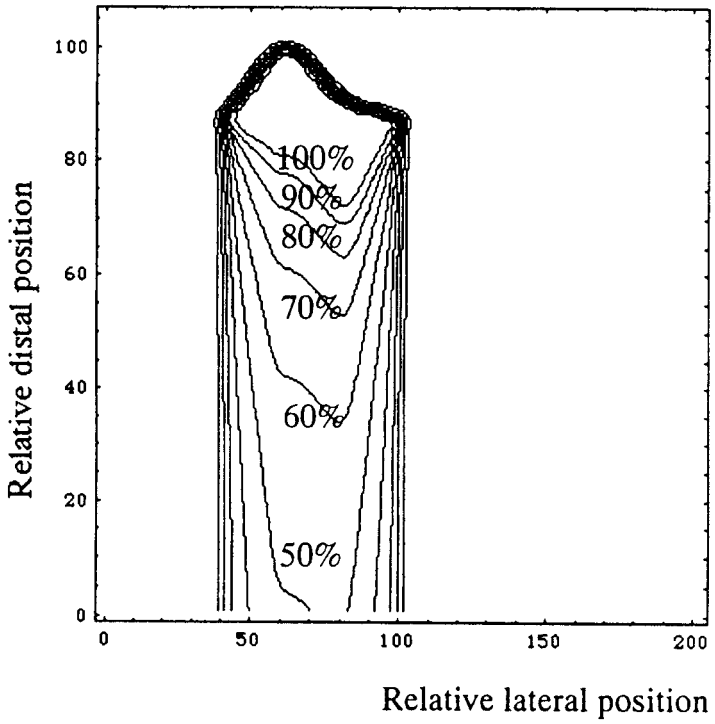

Figure 7. Isocontour plot of the optimized dose distribution.

optimized dose distribution (full curve) and a monoenergetic Bragg curve (dots), indicating that the optimization minimizes the distal dose fall-off while providing a homogeneous dose distribution inside the target.

Figures 6(*a*)–(*d*) show three-dimensional plots of the dose distribution during the optimized irradiation, while figure 7 gives an isocontour plot of the final dose distribution. Although we have optimized the dose distribution only in a depth direction, the lateral dose fall-off was also practically optimized due to the target shape characteristic. We suggest that for most convex cancer targets the proposed optimization works well for broad beam three-dimensional proton therapy with an advantage of minimized distal and lateral fall-off. The one-dimensional GSPM calculation time using a Power Macintosh 8100/100 MHz was of the order of 10 s depending on the number of beams considered.

4. Discussion

In this report we show preliminary results using homogeneous water phantom models. However, once we calculate spatially varying energy deposition kernels using Monte Carlo methods or other analytical approximations such as semi-infinite slab models, it is possible to perform dose optimization in a heterogeneous body using the GSPM method. We have demonstrated one-dimensional examples followed by an application to the broad beam therapy system; however, the approach can be directly applied to a general three-dimensional spot scanning method (Kanai *et al* 1980, 1983b). The dose optimization for the three-dimensional spot scanning in heterogeneous media will be reported elsewhere. The GSPM procedure can also be applied to dose optimization of other radiotherapy means including photon, electron and heavier charged ions by considering RBE.

Acknowledgments

The authors are grateful to M Maeda, H Tsuchidate, T Oichi, T Nakanishi, S Nakamura, and K Nakanishi for their support and encouragement. The first author also wishes to thank anonymous referees for many valuable comments and suggestions.

References

Brahme A, Källman P and Lind B 1989 Optimization of proton and heavy ion therapy using an adaptive inversion algorithm *Radiother. Oncol.* **15** 189–97

Brahme A, Lax I and Andreo P 1981 Electron beam dose planning using discrete Gaussian beams *Acta Radiol. Oncol.* **20** 147–58

Goitein M and Sisterson J M 1978 The influence of thick inhomogeneities on charged particle beams *Radiat. Res.* **74** 217–30

Kanai T, Kawachi K, Kumamoto Y, Ogawa H, Yamada T, Matsuzawa H and Inada T 1980 Spot scanning system for proton radiotherapy *Med. Phys.* **7** 365–9

Kanai T, Kawachi K, Matsuzawa H and Inada T 1983a Broad beam three-dimensional irradiation for proton radiotherapy *Med. Phys.* **10** 344–6

——1983b Three-dimensional beam scanning for proton therapy *Nucl. Instrum. Methods* **214** 491–6

Larsson B 1961 Pre-therapeutic physical experiments with high energy protons *Br. J. Radiol.* **34** 143–51

Larsson T 1987 Absorbed dose calculations and dose planning with proton beams using a Gaussian pencil beam *Uppsala University School of Engineering, Department of Technology: Report Series* UPTEC 87116 E

Lind B 1988 Comparison of algorithms for solving inverse problems in radiotherapy *Book of Abstracts VIII ICMP (San Antonio, Texas)* paper MP 5.6

——1990 Properties of an algorithm for solving the inverse problem in radiation therapy *Inverse Probl.* **6** 415–26

Midorikawa Y, Ogawa J, Doi T, Hayano S and Saito Y 1997 Inverse analysis for magnetic field source searching in thin film conductor *IEEE Trans. Magn.* **33** 4008–10

Pedroni E 1995 The 200-MeV proton therapy project at the Paul Scherrer Institute: conceptual design and practical realization *Med. Phys.* **22** 37–53

Russell K, Grusell E and Montelius A 1995 Dose calculation in proton beams: range straggling corrections and energy scaling *Phys. Med. Biol.* **40** 1031–43

Saito Y, Itagaki E and Hayano S 1990 A formulation of the inverse problems in magnetostatic fields and its application to a source position searching of the human eye fields *J. Appl. Phys.* **67** 5830–2

Saito Y and Yoda K 1996 Method for generating energy distribution *Japanese Patent Application* 408315279

Saotome H, Coulomb J-L, Saito Y and Sabonnadiere J-C 1995 Magnetic core shape design by the Sampled Pattern Matching method *IEEE Trans. Magn.* **31** 1976–9

Saotome H, Kitsuta K, Hayano S and Saito Y 1993 A neural behaviour estimation by the generalized correlative analysis *IEEE Trans. Magn.* **29** 1389–94

Scheib S, Pedroni E, Lomax A, Blattman H, Böhringer T, Coray A, Lin S, Munkel G, Schneider U and Tourovsky A 1994 Spot scanning with protons at PSI: experimental results and treatment planning *Hadrontherapy in Oncology* ed U Amaldi and B Larsson (Amsterdam: Elsevier) pp 471–80

Yoda K, Oka T, Tsutaka Y, Usami T, Nakamura H and Umeda Y 1997 Shape estimation of radioactive spent resins in a storage tank using the Sampled Pattern Matching *IEEE Trans. Nucl. Sci.* **44** 1469–73

Wolfram S 1991 *Mathematica, a System for Doing Mathematics by Computer* (San Francisco: Addison Wesley)

K.Yoda Dose optimization Pys.Ned.Baio 1997